MINISTÉRIO DA EDUCAÇÃO
INSTITUTO FEDERAL DE EDUCAÇÃO, CIÊNCIA E TECNOLOGIA DO RIO GRANDE DO SUL

Programa de Pós-Graduação em Tecnologia e Engenharia de Materiais
PPGTEM

DESENVOLVIMENTO DE UMA LIGA DE BAIXO CUSTO APLICADA AO FERRO FUNDIDO NODULAR AUSTEMPERADO ATRAVÉS DO AUXÍLIO DE REDES NEURAIS

DIOGO HOFMAM

CAXIAS DO SUL
2022

DIOGO HOFMAM

DESENVOLVIMENTO DE UMA COMPOSIÇÃO QUÍMICA DE BAIXO CUST APLICADA AO FERRO FUNDIDO NODULAR AUSTEMPERADO ATRAVÉS DO AUXÍLIO DE REDES NEURAIS

Dissertação apresentada ao Programa de Pós-Graduação em Tecnologia e Engenharia de Materiais para obtenção do grau de Mestre Profissional em Tecnologia e Engenharia de Materiais.

Área de Concentração: Tecnologia e Engenharia de Materiais

Linha de Pesquisa: Tecnologia da Transformação de Materiais

Orientador: Cleber Rodrigo de Lima Lessa

Coorientador: Guilherme V. B. Lemos

CAXIAS DO SUL

2022

Dados Internacionais de Catalogação na Publicação (CIP)

H713d Hofmam, Diogo

Desenvolvimento de uma composição química de baixo custo aplicada ao ferro fundido nodular austemperado através do auxílio de redes neurais / Diogo Hofmam ; orientador Cleber Rodrigo de Lima Lessa ; co-orientador Guilherme V. B. Lemos. – Caxias do Sul, 2022.

ix, 41 f. : il.

Dissertação (mestrado) – Instituto Federal de Educação, Ciência e Tecnologia do Rio Grande do Sul – Campus Caxias do Sul. Programa de Pós-Graduação em Tecnologia e Engenharia de Materiais. Mestrado Profissional em Tecnologia e Engenharia de Materiais. Caxias do Sul, 2022.

1. Ciência dos materiais. 2. Ferro fundido nodular. 3. Propriedades mecânicas. 4. Tratamento térmico – Austêmpera. 5. Redes neurais artificiais. I. Lessa, Cleber Rodrigo de Lima. II. Lemos, Guilherme V. B. III. Título.

CDU 669.13

Ficha catalográfica elaborada pela bibliotecária Núbia Marta Laux – CRB 10/1680

RESUMO

O presente trabalho apresenta o desenvolvimento de uma composição química de baixo custo para a produção de um ferro fundido nodular austemperado (ADI) que atenda a norma ASTM A897/897M – 2016 Grade 2 1050/750/07, atendendo as propriedades mecânicas de resistência à tração, resistência ao escoamento e alongamento, com o auxílio de redes neurais artificias. Através de extensa análise de composições químicas e propriedades mecânicas encontradas na literatura, foram compiladas informações para inserir em redes neurais, buscando uma otimização na relaçãoentre composição química, propriedades mecânicas e custo para a produção daliga desejada. Com base na composição química obtida, foi feito a fusão e posterior tratamento térmico do material. Com o material produzido, o mesmo foiusinado e testes mecânicos e metalográficos como ensaio de tração, dureza, análise via microscopia óptica, análise de microscopia por varredura e difração de raio x foram executados. Como resultado, foi compreendido que as redes neurais artificiais podem ser utilizadas para auxiliar na produção de um ADI que alcance valores de propriedades de acordo com padrões normatizados, com resultados atingindo ao exemplo de 1225 MPa de resistência à tração, 892 MPa de resistência ao escoamento, 10% de alongamento e com custo consideravelmente menor diante de seus concorrentes, gerando assim economia global de até 49%. Desta forma uma menor quantidade de recursos naturais utilizados para a produção de uma liga de baixo custo pode ser utilizada, atingindo as propriedades mecânicas e microestruturais desejadas.

Palavras-chave: Ferro Fundido Nodular Austemperado; Propriedades Mecânicas; Redes Neurais Artificiais; Redução de Custo.

ABSTRACT

This paper presents the development of a low-cost chemical composition for the production of an austempered nodular cast iron (ADI) that meets the ASTM A897/897M - 2016 Grade 2 1050/750/07 standard, meeting the mechanical properties of tensile strength, yield strength and elongation, with the aid of artificial neural networks. Through extensive analysis of chemical compositions and mechanical properties found in the literature, information was compiled to insert into neural networks, seeking an optimization in the relationship between chemical composition, mechanical properties and cost for the production of the desired alloy. Based on the chemical composition obtained, the melting and subsequent heat treatment of the material was performed. With the produced material, it was machined and mechanical and metallographic tests such as tensile test, hardness, optical microscopy analysis, scanning microscopy analysis and x-ray diffraction were performed. As a result, it was understood that artificial neural networks can be used to assist in the production of an ADI that achieves property values in accordance with standardized standards, with results reaching for example 1225 MPa tensile strength, 892 MPa yield strength, and 10% elongation, at a considerably lower cost compared to its competitors, thus generating global savings of up to 49%. In this way a smaller amount of natural resources used for the production of a low-cost alloy can be used, achieving the desired mechanical and microstructural properties.

Keywords: Austempered Ductile Iron; Mechanical properties; Artificial neural networks; Cost reduction.

SUMÁRIO

LISTA DE FIGURAS

ANEXO

LISTA DE TABELAS

ARTIGO 1 - USING ARTIFICIAL NEURAL NETWORK AS A TOOL FOR PRODUCING AN AUSTEMPERED DUCTILE IRON

ARTIGO 2 - ANALYSIS OF ADI MANUFACTURING FROM LOW-COST CHEMICAL COMPOSITION ALLOY

ANEXO

INTRODUÇÃO

Os ferros fundidos nodulares austemperados, da sigla em inglês, *ADI – Austempered Ductile Iron*, constituem uma classe de materiais brutos de fusão que passam pelo processo térmico de austêmpera. Como resultado, são obtidos materiais com ótimos resultados de resistência mecânica, resistência ao escoamento e satisfatória relação entre alongamento e tração (1,2).

O ADI encontra grande aceitabilidade no mercado consumidor devido a seu baixo custo de produção, ótima razão entre peso e resistência, aliado a ótimos resultados mecânicos, tanto para a indústria agrícola, automotiva, rodoviária e outras. Como um exemplo, uma parede de 3 mm de ADI pode substituir uma parede de 8-10 mm de uma parede em alumínio. O ADI tem um custo de 25-50% menor de compra quando comparado ao alumínio (3).

Considerando o processo de fusão do material, é de fundamental importância uma boa qualidade de matéria prima para a fusão. Em alguns casos são adicionados elementos tais como níquel, molibdênio e cobre, estes os quais para a produção do ADI são utilizados prioritariamente para aumentar a temperabilidade do material, gerando pouca interferência em resultados mecânicos (4,5).

O molibdênio pode ser necessário para peças fundidas com grandes secções transversais devido ao seu elevado grau de endurecimento. Com a presença de até 0,3% em liga, este elemento químico pode levar à precipitação de carbonetos durante a solidificação devido à sua tendência à segregação, desta forma é importante ser utilizado estritamente a quantidade necessária para atingir os resultados desejados. O cobre melhora o alongamento e a energia de impacto, aumentando a temperabilidade do material com até 0,8% de utilização em liga. Valores acima que reduzem a temperabilidade, ductilidade e resistência. O níquel por sua vez, aumenta a resistência e ductilidade, sendo este, o terceiro elemento com a maior capacidade de endurecimento (3-5).

O processo de austêmpera é um processo de tratamento térmico isotérmico e é feito através do aquecimento acima da zona crítica e mantido nesta temperatura até a uniformidade de temperatura no material. Após isso é colocado em um banho de sais fundidos em temperaturas entre 340°C – 380°C por um tempo determinado até atingir a microestrutura desejada (6,7).

Dessa forma, atinge-se o campo de formação da estrutura ausferrítica, microestrutura formada por agulhas de ferrita acicular ao redor do nódulo de gráfica em uma matriz de austenita estabilizada (7).

Quando o material sofre uma força aplicada pontualmente, neste local pode ser gerada uma estrutura de característica martensítica não revenida. Este efeito aumenta drasticamente a microdureza, aumentando consideravelmente a sua resistência à abrasão. Da mesma forma, o aumento de tensão compressivo na superfície, permite um alto grau de resistência à fadiga (8,9).

Tais materiais são normatizados via norma ASTM A897/897M – 16, permitindo um acordo entre fornecedor e cliente quanto a composição química do material, subdivididos em cinco classes as quais de forma mandatória indicam valores mínimos para resistência à tração (MPa), resistência ao escoamento (MPa), alongamento (%) e de forma apenas indicativa, dureza em escala Brinell. Desta forma, temos a Grade 1 – 900/650/09, Grade 2 – 1050/750/07, Grade 3 – 1200/850/04, Grade 4 – 1400/110/02 e Grade 5 – 1600/1300/01 (10).

Redes neurais artificiais, do inglês *ANN – Artificial Neural Network*, apresentam grandes vantagens em sua utilização como auto aprendizado e correlação entre seus resultados de saída (output). São modelos matemáticos que simulam o comportamento do sistema neural biológico. A utilização desta técnica pode prever possíveis resultados em variados tipos de processos e dessa forma permitir que os mesmos sejam otimizados antes de sua produção (11).

A arquitetura da rede (Figura 1) consiste em chamados nós ou neurônios, os quais realizam cálculos onde sua resultante de saída será a entrada da próxima camada, e assim consequentemente até a camada final (12).

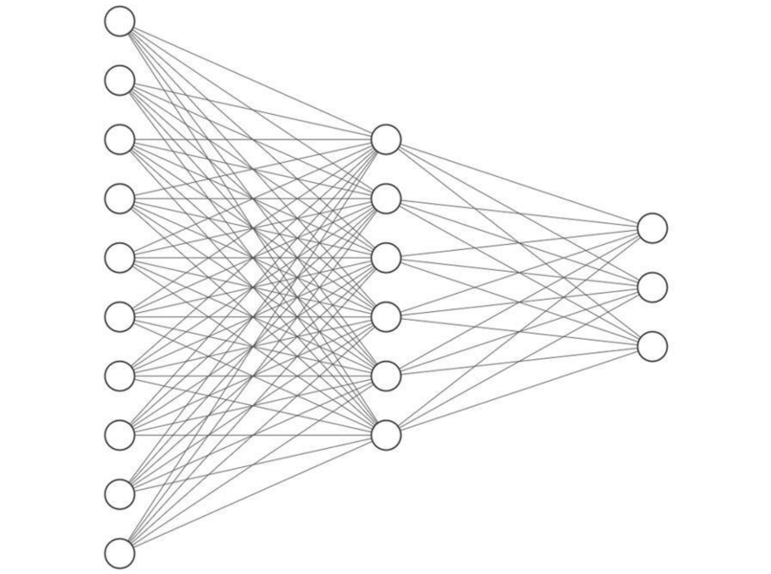

Figura 1. Arquitetura genérica de uma rede neural artificial.

O algoritmo de treinamento e sua arquitetura devem ser cuidadosamente selecionados para um melhor resultado, com sinais unidirecionais ou com forma de retro propagação, aprendendo desta forma consigo mesmo e desta forma minimiza o erro ajustando os pesos de cada camada, então sendo de ótima utilização paraproblemas com comportamentos não lineares (13,14).

Entre os modelos de rede neural utlizados para esta aplicação, temos o modelo de grande aceitabilidade chamado MLP (Perceptron Multicamadas) e esta rede é treinada com algoritmo de retro propagação na qual cada camada tem uma função definida e recebe informação da camada desaída (11,15).

O trabalho a seguir busca através do auxílio de redes neurais artificiais, o desenvolvimento de uma liga para a produção de um ferro fundido nodular austemperado que atenda a norma ASTM A897/897M – 16 Grade 2 1050/750/07 de baixo custo e favoráveis resultados metalúrgicos e mecânicos (10).

JUSTIFICATIVA E PROBLEMA

O ferro fundido é um material com grande aplicação no mercado consumidor devido a suas propriedades mecânicas, possibilidade de fundição nas mais variadas formas e de relativo baixo custo para produção.

Tendo em vista essa premissa, quando analisado o âmbito dos ferros fundidos nodulares, uma classe de material chama atenção, o dos ferros fundidos nodulares austemperados. Estes materiais após passarem pelo processo de tratamento térmico de austêmpera, ganham propriedades mecânicas que os permitem competir com outros tipos de materiais e suas aplicações, substituindo em alguns casos aços.

Devido aos crescentes aumentos de preço de matérias primas em nosso mercado nacional, tornou-se necessário a busca de materiais com baixo custo de produção que atendam as normas vigentes. Atrelado a isso, a utilização de redes neurais para dimensionar sua composição química, levando em conta a inteligência artificial, a arquitetura de rede e algoritmo de aprendizagem, vem ao encontro com a possibilidade de uma maior assertividade na produção do mesmo.

OBJETIVOS

Este trabalho se propôs a atender ao objetivo geral e aos objetivos específicos a seguir.

Objetivo geral

Desenvolvimento de uma composição química, de baixo custo, para a produção de um ferro fundido nodular austemperado, que atenda as normas, com o auxílio de redes neurais artificiais.

Objetivos específicos

- Obter através de referencial teórico, composições químicas e dados sobre propriedades mecânicas para ferros fundidos nodulares austemperados, dessa forma obtendo dados para alimentar a rede neural.
- Buscar o desenvolvimento de uma liga que atenda a norma vigente ASTM A897/897M – 16 Grade 2 1050/750/07.

- Produzir um ferro fundido nodular austemperado.

- Executar ensaios mecânicos e metalográficos para posterior comparação com os resultados previstos pela rede neural.

- Obter uma composição química com baixo uso de elementos de liga, a fim de diminuir o consumo de recursos naturais.

- Obter um material com baixo custo de produção competitivo dentro do mercado consumidor.

ESTRUTURA DO TRABALHO

Este trabalho foi estruturado em três partes, sendo elas, artigo um, artigo dois e conclusão.

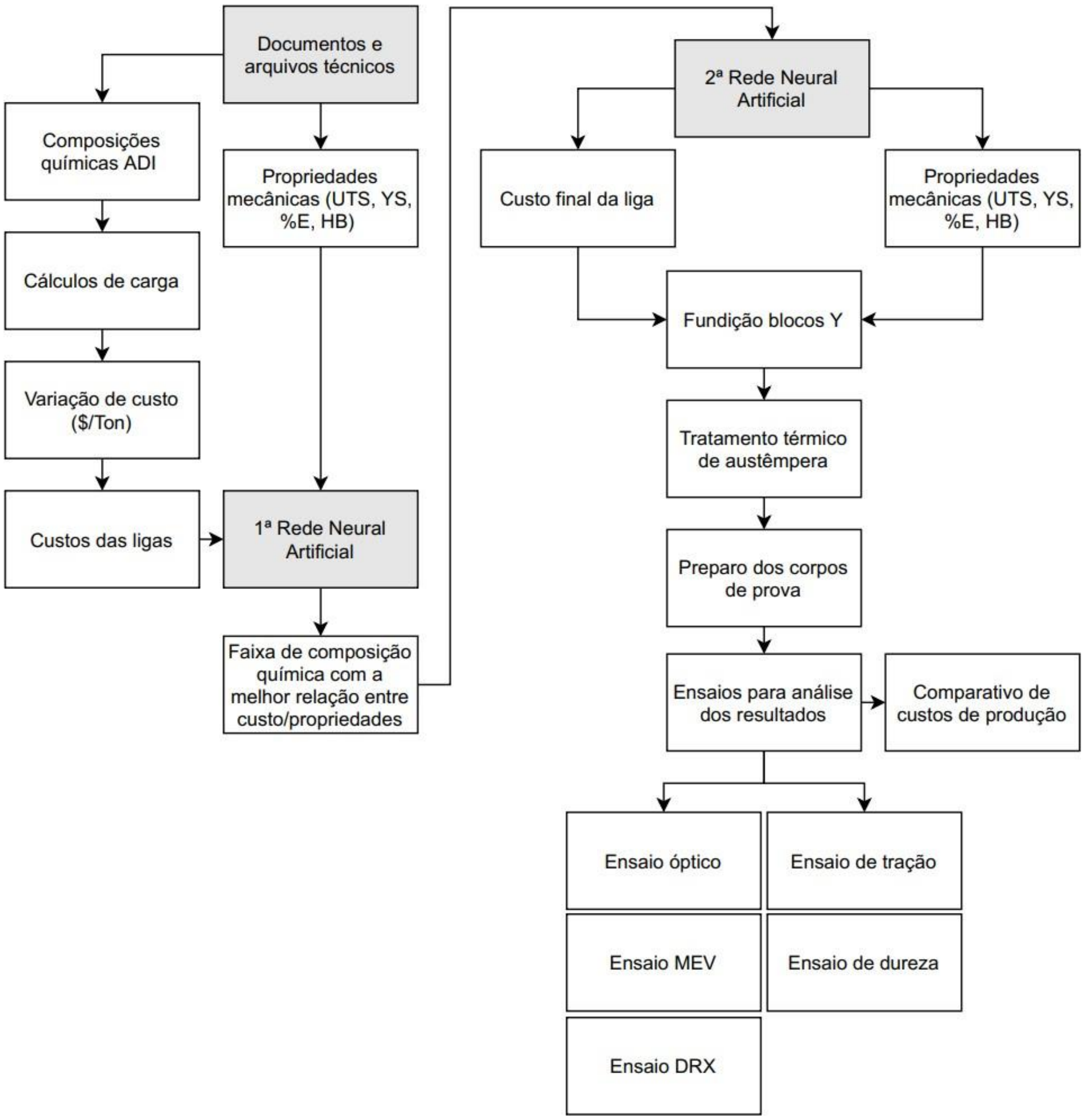

Figura 2. Fluxograma da formação do trabalho.

O fluxograma demonstrado acima, apresenta o fluxo de processo para a formação deste trabalho. Em primeiro momento será pesquisado um banco de dados através da literatura onde, com base nos documentos abordados, será separado a composição química e propriedades mecânicas encontradas pelos autores. Após isto, e utilizando cálculo de carga, será obtido os custos para produção destas composições químicas para desta forma obter os dados de entrada para a primeira rede neural.

A primeira rede neural irá resultar em uma faixa de composição química com a melhor relação entre custo e propriedades mecânicas. Contando com este resultado, uma segunda rede neural resultará no custo final da liga, bem como as propriedades mecânicas estimadas para este material.

Na etapa seguinte, será fundido o material em blocos Y de acordo com norma ASTM A536 - 14 e executado o tratamento termoquímico de austêmpera com base na norma ASTM A897/897M - 16 .

Com o material já processado, inicia-se a etapa de preparo dos corpos de prova, com corte, usinagem e preparo metalográfico, para serem analisados as resultantes mecânico metalúrgico do processamento. Entre os ensaios para análise microestrutural, temos, análise por via óptica, microscopia eletrônica de varredura e difração de raio X. Para análise de suas propriedades mecânicas, temos o ensaio de tração e de dureza.

Por fim, é feito um comparativo de custos de produção para verificar a competitividade entre o material produzido frente aos encontrados na literatura.

ARTIGO 1 - ARTIFICIAL NEURAL NETWORKS FOR PRODUCING A LOW-COST AUSTEMPERED DUCTILE IRON

ARTIFICIAL NEURAL NETWORKS FOR PRODUCING A LOW-COST AUSTEMPERED DUCTILE IRON

Diogo Hofmam[1, *]; Fabiano Dornelles Ramos[2, 4]; Guilherme Vieira Braga Lemos[3, 4]; Cleber Rodrigo de Lima Lessa[1, 2.]

[1] Programa de Pós-Graduação em Tecnologia e Engenharia de Materiais PPG-TEM do Instituto Federal do Rio Grande do Sul (IFRS), Caxias do Sul, Brasil.
[2] Instituto Federal do Rio Grande do Sul (IFRS), Caxias do Sul, Brasil.
[3] Universidade Federal de Santa Maria (UFSM), Cachoeira do Sul, Brasil
[4]Programa de Pós-Graduação em Engenharia de Minas, Metalúrgica e de Materiais (PPGE3M), Universidade Federal do Rio Grande do Sul (UFRGS), Porto Alegre, Brasil
** Corresponding author: diogo.hofmam@outlook.com*

ABSTRACT

Two artificial neural networks (ANNs) were developed for producing an austempered ductile iron (ADI) with low-cost chemical composition and mechanical properties as per ASTMA897/897M-16-grade-1050/750/07 standard. Thus, the first ANN predicted the chemical composition range within the lowest cost and required mechanical properties. Next, in the second ANN, the resulting values from the first ANN were refined considering the target chemical composition suggested in the standard. Moreover, mechanical properties and microstructural analyses were undertaken in the ADI produced to support the ANNs' findings. Hence, ANNs can be used to make a standard-compliant ADI and achieve cost savings.

Keywords: Austempered ductile iron, Artificial neural network, Mechanical properties, Cost-savings.

INTRODUCTION

The mechanical properties of cast irons make them interesting for applications such as gearboxes, connecting rods, and wheel hubs, amongst others [1]. Overall, the microstructure of ductile cast iron (DCI) is composed by ferrite and pearlite with nodular graphite [2]. Besides, low-cost production with improved yield strength (YS) and ultimate tensile strength (UTS) through the austempering process can be reached [3]. The mechanical properties are classified in ASTM A897/A897M-16 [4] to ensure reliability for producing ADI. Thus, austempering process consists of austenitising at 815-925°C to generate an austenite microstructure (γ), followed by quenching at 260-400°C for the process to occur [5,6]. The resulting microstructure is acicular ferrite, which might be called ausferrite in a carbon saturated austenite matrix [7–10].

Artificial neural networks (ANN) can be used in varied engineering fields due to their excellent self-learning function. ANNs are a potential tool for forecasting various consequences of the manufacturing process [11,12]. Cao et al. [11] showed that the cutting force for machining an ADI was successfully estimated using ANN, with an error of around 4%. Hammood et al. [13] presented ANN for the effect of retained austenite on fatigue life, and the mechanical properties were predicted with high accuracy. Guo [14] analysed the hardness through ANN and varied austempering parameters, and thus the predicted values approached the measured data. Ławrynowicz et al. [15] compared the mechanical properties of ADI through an algorithm showing that ANN is suitable for analysing the ultimate tensile strength (UTS), yield strength (YS), and elongation.

The current work aims at producing an ADI with low-cost chemical composition and required mechanical properties by applying ANNs. Thus, these mechanical properties are as per ASTM A897/897M - 16 Grade 2 1050/750/07 standard.

MATERIALS AND METHODS

Database

The current investigation was based on reports and technical sheets related to ADI production [19–40]. The database was organised with a variation in the chemical compositions (low to high levels of alloying elements) seventy-five chemical compositions with thirteen alloying elements (C, Si, Mn, Mo, Ni, Mg, S, Cu, Cr, Ti, Al, V, Nb) and their mechanical properties (UTS) [MPa], YS [MPa], elongation [%], and hardness Brinell [HB]). All these are required following ASTM A897/897M-16. So, this database was used for calculating the furnace charge and estimating the cost variation [$/ton].

The furnace charge, cost variation, and dataset

The charge calculation estimated a minimum of a ton of cast iron for each alloy [43]. The primary raw materials were pig iron, steel scrap, and ferroalloys. To that, the data from the international market [44] and the Brazilian Foundry Association [45] were used, and quantities for producing cast iron in the charge, and the gross cost was estimated [45,46]. Therefore, the alloy cost was obtained by its variation between different charges. The minimum cost was identified as "100%", up to a maximum of "472.71%". Thus, a dataset containing variables as costs in charge and chemical compositions with their mechanical properties (C, Si, Mn, Mo, Ni, Mg, S, Cu, Cr, Ti, Al, V, Nb, cost variation [$/ton], YS, UTS, %E, and HB), totaling 1350 pieces of information. Table 1 shows a significant price variation.

Table 1. Cost variation (%) between chemical compositions.

Sample	1	2	3	...	72	73	74	75
%	100.00%	102.76%	103.11%	...	257.79%	289.45%	359.41%	472.71%

Artificial neural network models, inputs, and outputs

An ANN model involves computations and mathematics for simulating the human–brain processes. ANNs have a specific architecture format, and regression models between data collection and analysis, structure design, hidden layers, simulation, and weights/bias trade-off computed through learning and training methods. Using an error optimisation algorithm (Levenberg-Marquardt (LMT), the ANN could find optimum weight for each synapse (the connection between nodes of different layers) after a certain number of epochs. Once the ANN is successfully trained, input parameters can be fed into the model, and afterwards, the ANN can predict the output parameters. In the current investigation, the ANN models were made using MATLAB software. The architecture of the LMT algorithm had multiple layers of the backpropagation type, which led to a superior performance in heat treatment [16]. The mean square error (MSE) was calculated using:

$$MSE = \frac{1}{N}\sum_{i=1}^{N}(f_i - y_i)^2$$

where N is the number of data points, fi is the value returned by the model, and yi is the actual value for data point "i". The MSE was obtained from the ANN training session.

The calculation of the partial derivatives of error concerning the parameters of the ANN is essential [17]. Thus, the accuracy (R2) was used as a good indicator; when R2 was close to 1, it meant maximum accuracy [18].

The first ANN was designed and trained using the LMT algorithm from the dataset information. Therefore, the LMT algorithm correlated the data by cross-referencing them using 70% for training, 15% for validation, and 15% for testing with these percentages based on [41,42]. The first ANN was constructed using minimum values simulated according to the standard (UTS 1050 MPa, YS 750 MPa, %E ~7, 302 HB, and $/ton < 100% (in Table 1); thus, the minimal requirements of these properties could lead to the lowest ADI cost. The minimum values were tested sixty-five times, which resulted in a certain range for each element. The first ANN is shown in Figure 1, and its architecture containing one hidden layer with seventeen nodes is next presented in Figure 2. Moreover, the second ANN is also shown in Figure 1, and its architecture comprising one hidden layer with seventeen nodes is further displayed in Figure 3.

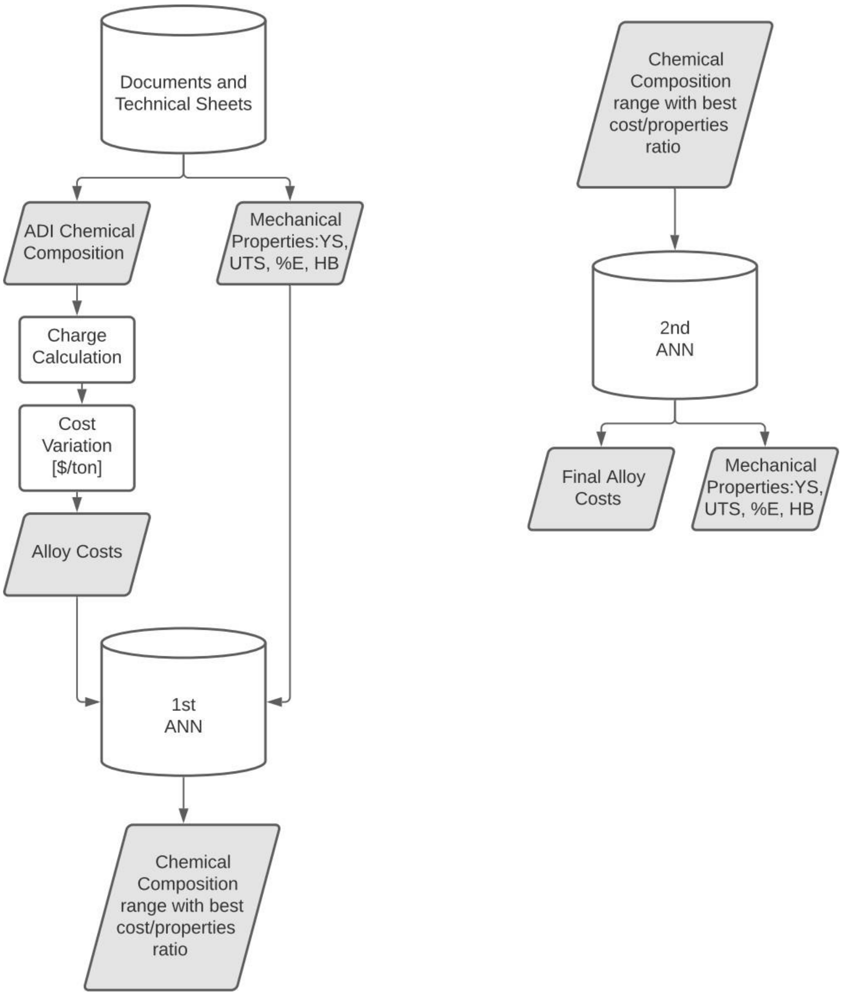

Figure 3. Flowchart showing the two ANNs of this work.

In Figure 2, the architecture of the first ANN shows five input data values (UTS, YS, %E, HB, and $/ton). Therefore, this ANN contained one hidden layer with seventeen nodes and thirteen output element values (chemical composition).

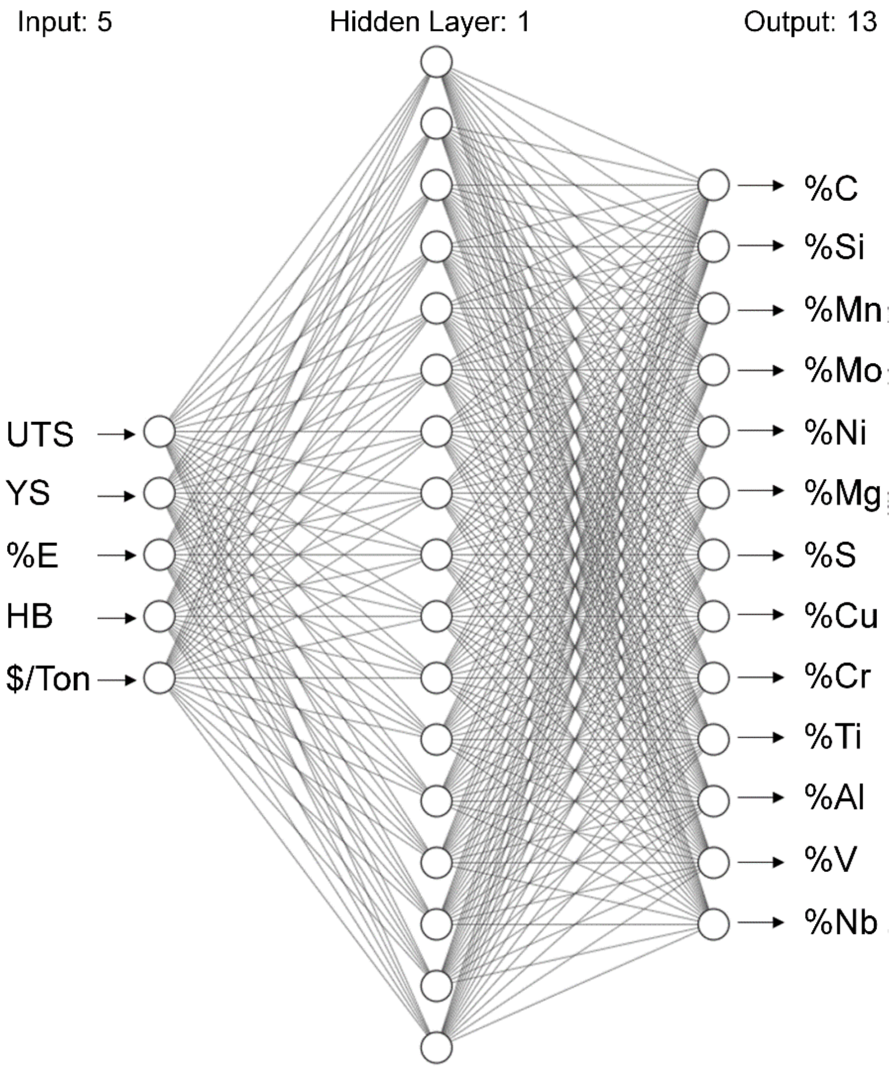

Figure 4. Architecture of the 1stANN.

Figure 3 shows the second ANN, where the input layer was the outcomes from the first ANN (chemical composition range tested), with one hidden layer, seventeen nodes, and five outputs (UTS, YS, %E, HB, and $/ton). The chemical composition range obtained in the first ANN (low and high quantities of alloying elements) was tested ten times at each level in the second ANN, thus equalling twenty trials. Thus, the second ANN was programmed to verify if the resulting chemical composition range of the first ANN implied a chemical composition that led to the required mechanical properties.

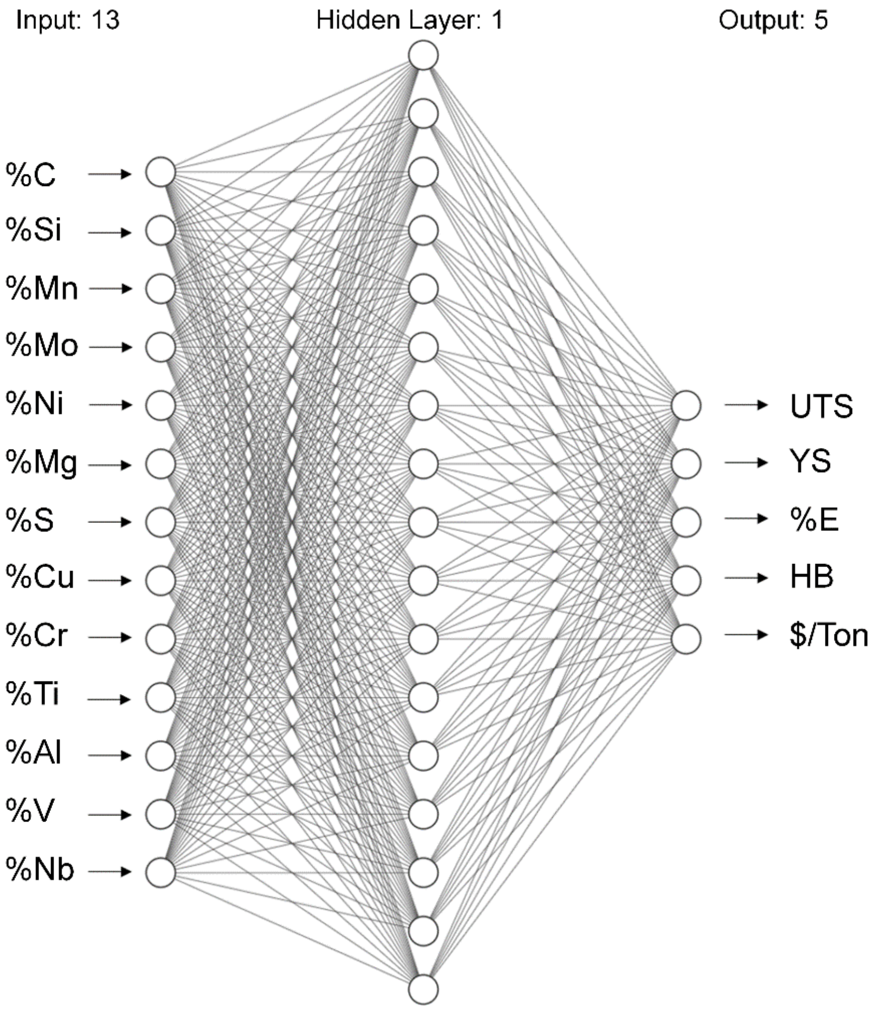

Figure 5. Architecture of the 2nd ANN.

Casting and heat treatment

The molten metal with the resulting chemical composition was prepared in an induction electric furnace Inductotherm with a 1500 kg/hr capacity. Five Y-blocks of 25 mm thickness were pouring, and their dimensions are displayed in Figure 4.

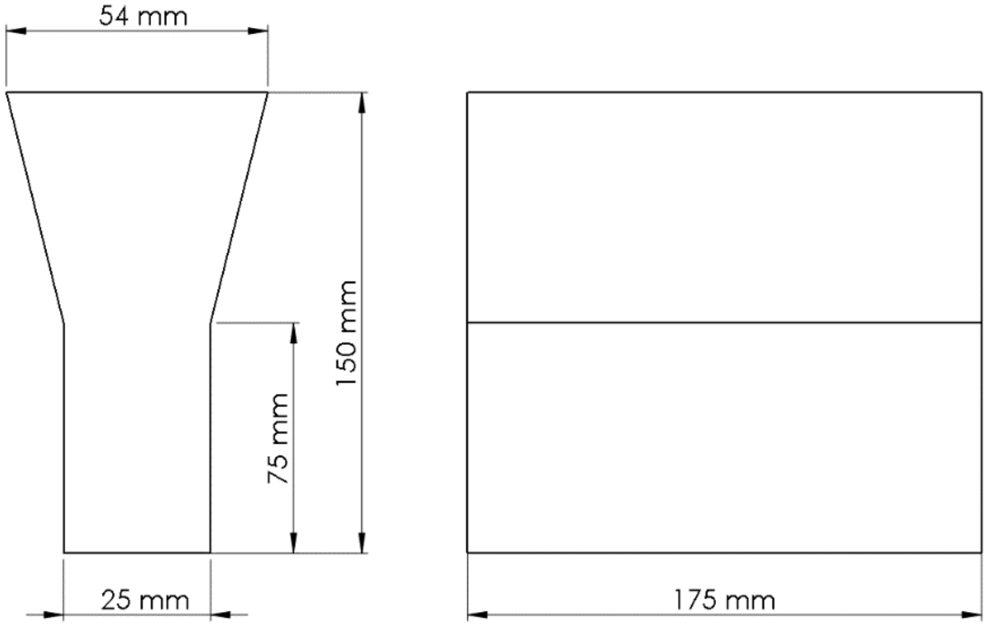

Figure 6. Y-block dimensions.

After casting, the five Y-blocks were heat treated. In this context, based on the literature [2, 19, 21, 27], the temperature for austenitisation was 850°C, and for austempering, it was 350°C. Considering these temperatures, the steps of the heat treatment were selected. Therefore, as shown in Figure 5, the alloy was austenitised for 30 minutes at 840°C (austenitising step) in a muffle furnace. After quenching, the austempering process was done for 30 minutes at 340°C in a quenching tank with a molten salt bath (sodium and potassium nitrate, NaNO3 + KNO3). Later, the samples were washed in hot water [47–49].

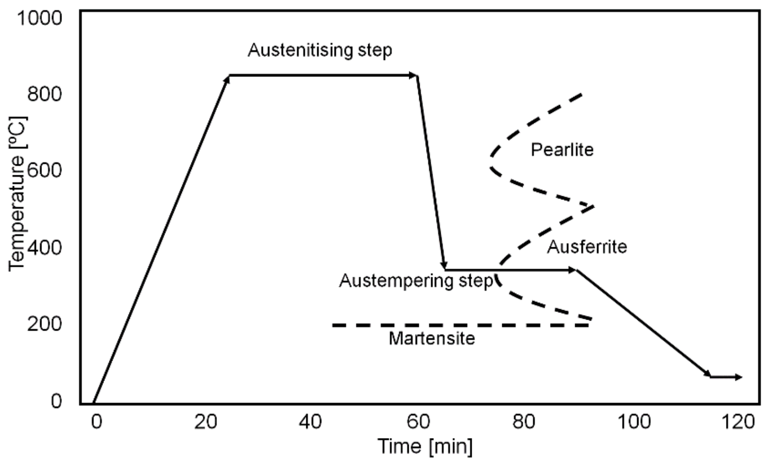

Figure 7. Heat treatment steps for ADI productions.

Samples with 58 mm length and 13 mm diameter were extracted for tensile tests, as per ASTM A897/A897M-16 [4]. Furthermore, hardness measurements were performed in a Brinell Hardness tester with a 3000 kg load, as indicated in ASTM A897/897M - 2016. Complementarily, microhardness tests were carried out on a Mitutoyo HV 100 machine with a 1-kilogram load (HV1) due to the resulting microstructure. Thus, five measurements were performed in the ausferrite phase, and an average and standard deviation were calculated.

For microstructure investigation, samples were cut, prepared according to metallography, and etched using 3% Nital. The microstructure was analysed by optical microscopy (OM) in an OLYMPUS and scanning electron microscopy (SEM) in a SHIMADSU SSX-550 [47]. In addition, the degree of nodularization was verified through comparison with images of [50]. Next, grain size and nodule count were measured using ImageJ software [51].

RESULTS AND DISCUSSION

In Table 2, the resulting chemical composition range verified in the first ANN is presented. The suitability of the models proposed can be demonstrated through the R2 scores achieved. Thus, Figure 6 shows that the R2 scores of the first ANN were above 98%.

Table 2. Chemical composition range in the 1stANN.

	%C	%Si	%Mn	%Mo	%Ni	%Mg	%S	%Cu	%Cr	%Ti	%Al	%V	%Nb
Min.	3.60	2.40	0.50	0.00	0.01	0.05	0.01	0.05	0.05	0.00	0.02	0.00	0.00
Max.	3.70	2.50	0.60	0.00	0.02	0.06	0.01	0.05	0.06	0.00	0.10	0.00	0.00

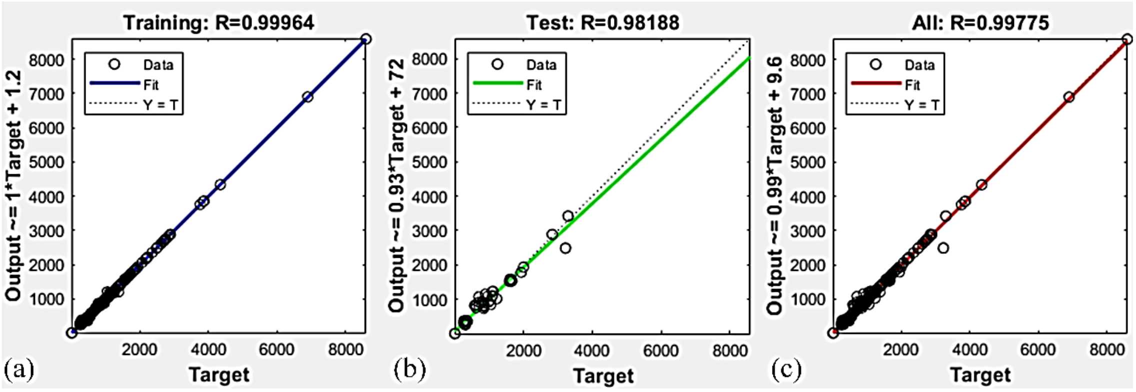

Figure 8. First ANN R2 scores (a) training 99.96%, (b) test 98.2% and (c) all 99.77%.

The chemical composition of ADI verified in the first ANN was evaluated by a spectrometer, and it is given in Table 3. In other words, the chemical composition predicted by the ANN was compared to that found in the ADI produced.

Table 3. Manufactured chemical composition ADI alloy (wt%).

	%C	%Si	%Mn	%Mo	%Ni	%Mg	%S	%Cu	%Cr	%Ti	%Al	%V	%Nb
Sample	3.69	2.42	0.54	0.00	0.01	0.05	0.01	0.02	0.05	0.00	0.02	0.00	0.00

Figure 7 presents the ausferrite phase, with characteristics such as needle-shaped acicular ferrite and stabilised austenite. Moreover, these results have similarities with the study of Mrzygłód B. [10], where an ADI was austenitised at 920°C and austempered in salt baths at varying temperatures including a similar as used in this investigation. However, it should be noted that the present work attempted the production of ADI with a low amount of alloying elements, which thus led to a lower final cost. Figure 7 (a) shows the graphite nodule, stabilized austenite, and acicular ferrite, as likewise seen by other authors [52-53]. Thus, in this way, our outcomes agree well with related studies on ADI [10, 52-53]. Figure 7 (b) presents SEM imaging analysis detailing the results shown in the OM. Finally, with graphite type I, the average nodule count was 362 nodules/mm2. In addition, the degree of nodularization was 95%, and the average size of graphite was 35.69 μm. Therefore, it is noted that these findings follow ASTM A247 – 17 [50].

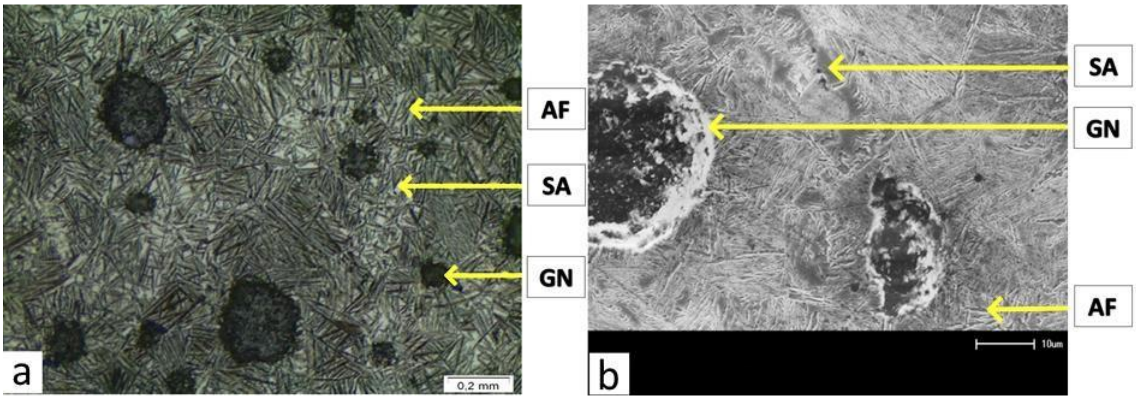

Figure 9. Microstructure observation (a) through optical microscope, where GNis Graphite Nodule, SA is Stabilized Austenite, and AF is Acicular Ferrite. (b) observation through SEM imaging.

In Figure 8, tensile testing results are shown by comparing the ADI produced, the standard, and three alloys found in literature [21, 27, 28], which works were selected as they reported an improvement in UTS due to the greater amount of ausferrite. However, Sellamuthu, P. and Jiwang Z. [2, 36] employed a great quantity of alloying elements, which would lead to high costs. Therefore, the non-necessity of high number of alloying elements for achieving desired mechanical properties affects the cost production. The ADI produced shows one of the highest in UTS, besides being up to 81.23% cheaper compared to the selected alloys [21, 27, 28]. In addition, the indicated hardness range for ASTM A897/897M – 2016 grade 2 considering the microstructure formed is 302-375 HB: the current work achieved 354 HB, which is suitable. Putanda K. S. [28] obtained a hardness like the ADI as our study but with a high amount of alloying elements, thus demonstrating the importance of this work. Furthermore, microhardness measurements were done in the ausferrite phase, thus achieving an average of 382 HV (σ ±9.633).

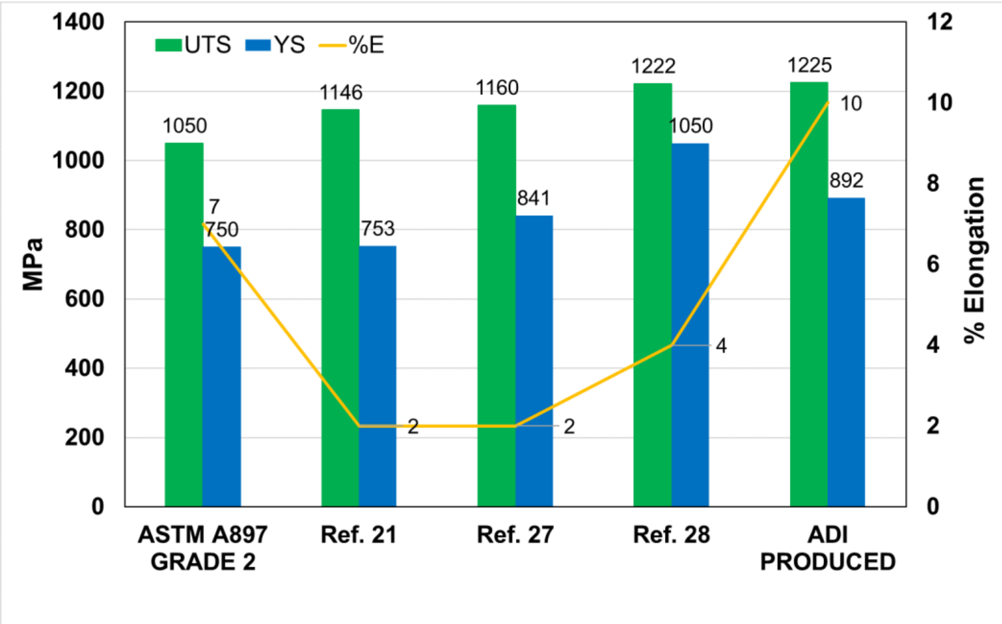

Figure 10. Comparison of mechanical properties between ADI produced, threereports from literature, and requirements of ASTM A897/897M – 16 Grade 2.

In Figure 9, the average cost of the alloys used for the ANN development was 49.8% higher than the cost of the ADI produced. Moreover, these values are also shown as the amount of Mo and Nb plays an essential role in cost savings. Therefore, the ADI manufactured was 6.2% cheaper than the minimum value of the alloy [54]. In addition, the most expensive alloy (maximum value) costs 372.7% [55] more than the ADI produced. Thus, a low-cost ADI was manufactured, with requirements of microstructure and mechanical properties as per the standard [4]. Furthermore, both quantities of Mo and Nb in the ADI produced were basically zero, which agrees with its lowest cost.

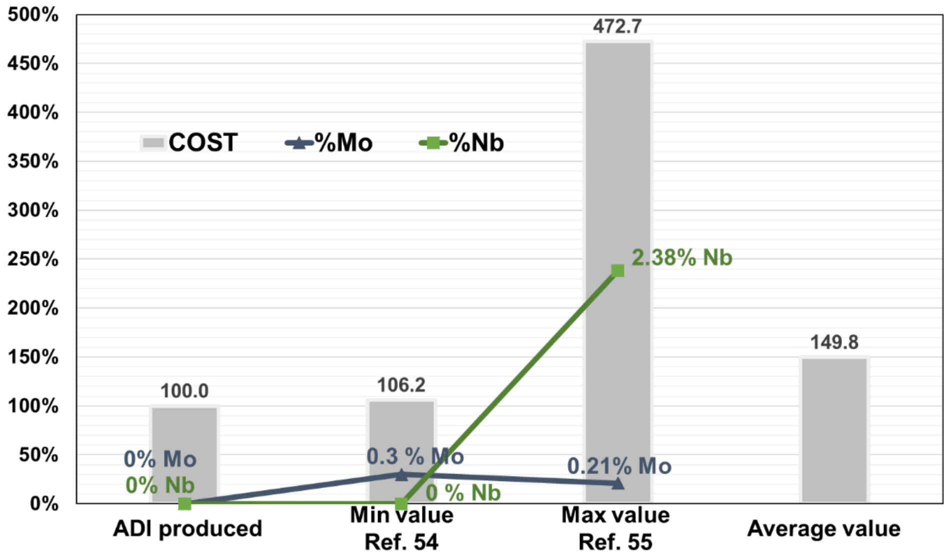

Figure 11. Cost comparison between alloys. Percentage (%) was defined as: ADI produced is 100%, and minimum and maximum values stand for the difference in relation to the ADI produced.

CONCLUSION

i) A low-cost chemical composition was predicted through artificial neural networks (ANNs) for producing an austempered ductile cast iron (ADI). Next, chemical composition and mechanical properties were analysed in the manufactured ADI. Therefore, the ADI produced met the requirements of the ASTM A897/897M – 16 Grade 2 1050/750/07 standard.

ii) The architecture of the first and second ANNs using the Levenberg–Marquardt algorithm (LMT) was effective for predicting a low-cost chemical composition, mechanical properties, and final cost of ADI. Furthermore, the microstructure of the ADI manufactured was characterised by ausferrite with stabilised austenite.

iii) An ADI was produced with a considerable cost reduction compared to the costs of the alloys used in the database for developing the ANNs. Thus, the ADI manufactured was around 49% cheaper than the average cost of the alloys considered. However, a cost reduction during manufacturing cast parts might be complex and should be analysed in each specific context.

REFERENCES

1. Korkmaz S. A methodology to predict fatigue life of cast iron: Uniform material law for cast iron. J. Iron Steel Res. Int. 2011;18(8):42–5.

2.Sellamuthu P, Samuel DGH, Dinakaran D, et. al. S. Austempered ductile iron (ADI): Influence of austempering temperature on microstructure, mechanical and wear properties and energy consumption. Metals. 2018;8(1).

3. Imasogie BI, Afonja AA, Ali JA. Properties of ductile cast iron nodularised with multiple calcium-magnesium based master alloy. Mater. Sci. Technol. 2000;16(2):194–201.

4. American Society for Testing and Materials (ASTM). Standard Specification for Austempered Ductile Iron Castings. West Conshohocken: ASTM; 2016. Standard No. A897/897M – 2016.

5. Cakir MC, Bayram A, Isik Y, et al. The effects of austempering temperature and time onto the machinability of austempered ductile iron. Mater. Sci. Eng. A. 2005;407(1–2):147–53.

6. Panneerselvam S, Putatunda SK, Gundlach R, et al. Influence of intercritical austempering on the microstructure and mechanical properties of austempered ductile cast iron (ADI). Mater. Sci. Eng. A. 2017;694:72–80.

7. Savangouder RV, Patra JC, Bornand C. Prediction of hardness of austempered ductile iron using enhanced multilayer perceptron based on Chebyshev expansion. Commun. Comput. Inf. Sci. 2019;414–22.

8. Wang B, Barber G, Sun X, et al. Characteristics of the transformation of retained austenite in austempered tempered ductile iron. J. Mater. Eng. Perform. 2017;26(5):2095–101.

9. Da Costa e Silva ALV, Mei PR. Aços e ligas especiais [Steels and special alloys]. São Paulo (SP): Blucher. 2021.

10. Mrzygłód B, Kowalski A, Olejarczyk-Wozenska I, et al. Characteristics of ADI ductile cast iron with single addition of 1.56% Ni. Arch. Metall. Mater. 2017;62(4):2273–80.

11. Cao D, Guo XH. Prediction of cutting force of austempered ductile iron based on BP neural network. Adv. Mat. Res. 2013;774–776:1068–74.

12. Moutarde PF. Introduction to (shallow) Neural Networks. Centre For Robotics

MINES ParisTech. 2021;1-22.
13. Ȧ ASH, Ḃ HML. A study the effect of retained austenite on fatigue life of austempering ductile iron by using artificial neural networks. Int. j. Curr. Eng. Technol. 2013;1–6.
14. Guo X. Correlation between austempering parameters and hardness of austempered ductile iron based on artificial neural network. Comput. Model. New Technol. 2014;18(3):72–6.
15. Ławrynowicz Z, Dymski S. Neural network analysis of tensile properties of austempered ductile iron. Adv. Mater. Sci. 2008;8(1).
16. Agbeleye A, Esezobor D, Agunsoye J, et al. Prediction of the abrasive wear behaviour of heat-treated aluminium-clay composites using an artificial neural network. J. Taibah Univ. Sci. 2018;27;12:1–6.
17. Biernacki R, kozłowski J, myszka D, et al. Prediction of properties of austempered ductile iron assisted by artificial neural network. Inst. Mater. Proc. 2006;12(1):11–5.
18. Masood Chaudry U, Hamad K, Abuhmed T. Machine learning-aided design of aluminum alloys with high performance. Mater. Today Commun. 2021;26:101897.
19. Kovacs B v. Development of austempered ductile iron (ADI) for automobile crankshafts. J. Heat Treat. Mater. 1987;5(1):55–60.
20. Putatunda SK, Singh I. Fracture toughness of unalloyed austempered ductile cast iron (ADI). J. Test. Eval. 1995;23(5):325–32.
21. Zimba J, Simbi DJ, Navara E. Austempered ductile iron: an alternative material for earth moving components. Cem. Concr. Comos. 2003;25:643–9.
22. Souza SAR. Influência do alumínio nas propriedades mecânicas do ADI (Austempered Ductile Iron) [Influence of aluminum on the mechanical properties of ADI (Austempered Ductile Iron)] [master's thesis]. Belo Horizonte (MG): Universidade Federal de Minas Gerais. 2004.
23. Shelton P, Bonner A. The effect of copper additions to the mechanical properties of austempered ductile iron (ADI). J Mater Process Technol. 2006;173:269–74.
24. Putatunda S, Kesani S, Tackett R, et al. Development of austenite free ADI (austempered ductile cast iron). Mater. Sci. Eng. A. 2006;435:112–22.

25. Si SP, Composites NS, Yang J, et al. Microstructure and Mechanical Properties of austempered ductile iron. Mater. Sci. Eng. C. 2001;12:406–12.
26. Kim Y-J, Shin H, Park H, et al. Investigation into mechanical properties of austempered ductile cast iron (ADI) in accordance with austempering temperature. Mater. Lett. 2008;62:357–60.
27. Junior ARM. Influência dos elementos de liga Cu-Ni-Mo nas propriedades mecânicas e na austemperabilidade do ADI [Influence of Cu-Ni-Mo alloying elements on the mechanical properties and austemperability of ADI] [master's thesis]. São Paulo (SP): Universidade de São Paulo. 2009.
28. Putatunda SK. Comparison of the mechanical properties of austempered ductile cast iron (ADI) processed by conventional and step-down austempering process. Mater. Manuf. 2010;25(8):749–57.
29. Basso A, Caldera M, Sikora J. Mechanical characterization of dual phase austempered ductile iron. ISIJ INT. 2010;50:302–6.
30. Sahoo S, Patnaik S, Sen S. A study on the effect of austempering temperature, time and copper addition on the tensile properties of austempered ductile iron. NCATAE 2011.
31. Mattar AR, Heck S, Lombardi A, et al. Influence of alloying elements Cu, Ni and Mo on mechanical properties and austemperability of austempered ductile Iron. Int. Heat Treat. Surf. Eng. 2011;5:78–82.
32. Guesser WL, Koda F, Martinez JAB, et al. Austempered ductile iron for gears. SAE Technical Papers. 2012.
33. Padan DS. Microalloying in austempered ductile iron (ADI). Trans Amer. Foundry. Soc. 2012;120(12–019):277–88.
34. Kowalskia A, S. K-N, Regulski K. ADI after austenitising from intercritical temperature. Arch. Foundry Eng. 2013;13.
35. Das A, Dhal J, Panda R, et al. Effect of alloying elements and processing parameters on mechanical properties of austempered ductile iron. J. Mater. Metal. Eng. 2013;3:8–16.
36. Zhang J, Zhang N, Zhang M, et. al. Microstructure and mechanical properties of austempered ductile iron with different strength grades. Mater. Lett. 2014;119:47–50.

37. Panneerselvam S, Martis CJ, Putatunda SK, et al. An investigation on the stability of austenite in austempered ductile cast iron (ADI). Mater. Sci. Eng. A. 2015;626:237–46

38. Basso A, Caldera M, Massone J. Development of high silicon dual phase austempered ductile iron. ISIJ inter. 2015;55(5):1106–13.

39. Méndez S, de la Torre U, González-Martínez R, et al. Advanced properties of ausferritic ductile iron obtained in as-cast conditions. Int. J. Met. 2016;11.

40. Olawale O, Ibitoye S, Oluwasegun K, Shittu M, et al. Forced-air cooling quenching: a novel technique for austempered ductile iron production. Int. J. Met. 2016;11.

41. Khan I, Raja MAZ, Shoaib M, et al. Design of neural network with Levenberg-Marquardt and Bayesian regularization backpropagation for solving pantograph delay differential equations. IEEE 2020;8(0):137918–33.

42. Lv C, Xing Y, Zhang J, et al. Levenberg-Marquardt backpropagation training of multilayer neural networks for state estimation of a safety-critical cyber-physical system. IEEE 2018;14(8):3436–46.

43. Seidu SO, Onigbajumo A. Development of charge calculation program for target steel in induction furnace. LEJPT. 2015;14(27):81–97.

44. FASTMARKETS [Internet]. London (UK). 2021 [cited 2021 Aug 10]. Available from: https://www.fastmarkets.com/commodities

45. ABIFA [Internet]. São Paulo (SP). 2021 [cited 2021 Sep 2]. Available from: https://abifa.org.br/

46. METAL BULLETIN [Internet]. London (UK) 2021 [cited 2021 Oct 28]. Available from: https://www.metalbulletin.com/steel/steel-raw-materials/ferrous/hbi-pig-iron-and-dri.html

47. Konca E, Tur K, Koç E. Effects of alloying elements (Mo, Ni, and Cu) on the austemperability of GGG-60 ductile cast iron. Metals. 2017;7:320.

48. Boccardo AD, Dardati PM, Celentano DJ, et al. Austempering heat treatment of ductile iron: computational simulation and experimental validation. Finite Elem. Anal. Des. 2017;134:82–91.

49. Boccardo AD, Dardati PM, Godoy LA, Celentano DJ. Sensitivity of austempering heat treatment of ductile irons to changes in process parameters.

Metall. Mater. Trans. B. 2018;49(3):1522–36.
50. American Society for Testing and Materials (ASTM). Standard test method for evaluating the microstructure of graphite in iron castings. West Conshohocken: ASTM; 2019. Standard No. A247 – 2019.
51. American Society for Testing and Materials (ASTM). Standard test methods for determining average grain Size. West Conshohocken: ASTM; 2010. Standard No. E112 – 2010.
52. Olawale JO, Ibitoye SA. Influence of casting section thickness on fatigue strength of austempered ductile iron. J. Mater. Eng. Perform. 2017;26(10):4997–5008.
53. Kutsov A, Taran Y, Uzlov K, et al. Formation of bainite in ductile iron. Mater. Sci. Eng. A. 1999;273–275:480–4.
54. Sellamuthu P, Samuel D.G. H, Dinakaran D, et al. Austempered ductile iron (ADI): influence of austempering temperature on microstructure, mechanical and wear properties and energy consumption. Metals. 2018;8:53.
55. Pimentel ASO, Guesser WL, Burbank J, et al. Abrasive wear behavior of austempered ductile iron with niobium additions. Wear 2019(440–441):203065.

ARTIGO 2 - ANALYSIS OF ADI MANUFACTURING FROM LOW-COST CHEMICAL COMPOSITION ALLOY

ANALYSIS OF ADI MANUFACTURING FROM LOW-COST CHEMICAL COMPOSITION ALLOY

Diogo Hofmam[1, *]; Cleber Rodrigo de Lima Lessa[1, 2.]

[1] *Programa de Pós-Graduação em Tecnologia e Engenharia de Materiais PPG-TEM do Instituto Federal do Rio Grande do Sul (IFRS), Caxias do Sul, Brasil.*
[2] *Instituto Federal do Rio Grande do Sul (IFRS), Caxias do Sul, Brasil.*

ABSTRACT

The continuous interest of the industry in the excellent mechanical properties performed by austempered ductile cast iron (ADI) combined with a low production cost compared with other metallurgical processes, an analysis of its optical and mechanical results becomes relevant. The ADI material ends up surpassing conventional cast iron and, in some cases, casting steel. From previous studies and based on the literature, a low-alloy ductile cast iron was produced and subsequently austempered heat treated. To analyze the results, optical microscopy (OM) and scanning electron microscopy (SEM) tests wereperformed. Mechanical tests were also carried out. Finally, an x-ray diffraction test was performed. As a result, it was found that it is possible to produce a material with low alloy and obtain extremely high gains in mechanical properties when compared to the as cast state. The micrography showed ausferrite formation in its structure as expected.

Keywords: Austempered Ductile Iron; Mechanical Properties; Austempering; Low-cost production.

INTRODUCTION

The austempered ductile cast iron is a material of great interest to the industry due to its excellent mechanical properties, cost benefit, being often cheaper to produce compared to its competitors, great strength and weight ratio. It is applied to various industries, such as the agricultural and automotive sectors (1–3).

From the production of a ductile cast iron and going through the heat treatment process of austempering, an ausferritic structure is generated. It is constituted by needles of acicular ferrite around the graphite and matrix with stabilized austenite. This combination generated by the heat treatment process includes this material in application fields once exercised by cast steels and occasionally in forged products (4–6).

The austempering process is an isothermal process, so it offers some advantages over materials that undergo through martensitic transformation, since this transformation takes place at different times in sections of differing section modulus. In this way, it can lead to cracks and fractures in the material while the austempering process takes place uniformly over a period of time (7,8).

The standard ASTM A897/897M determines the class of these materials, such as minimum mechanical properties, how the specimens should be dimensioned and separating them into grades (9).

Alloy elements are used in the austempered ductile cast iron in order to primarily increase the hardenability window of the material, having no primary influence on the behavior of other mechanical properties. The chemical elements most used in the literature are Nickel, Copper and Molybdenum, directly impacting the cost of producing the material. The first two, with low affinity with carbon and ferrite stabilizers, and molybdenum with high affinity with carbon, increasing hardenability and being a ferrite stabilizer (10–13).

The production of low-cost ADI becomes an interesting study, because based on a cheap material with excellent mechanical properties, a wide range for application is opened (14).

In this work, a ductile cast iron based on the literature was produced and analyzed, going through the austempering process and comparing its mechanical and microstructural properties in its as cast state and later in its austempered state. The heat treatment parameters were selected according to articles specialized in the process.

This article analyzed the microstructure through optical and electronic microscopy. The tests to assess the mechanical properties were based on tensile and hardness tests. For analysis of the present phases, X-ray diffraction was used. The production of this material was carried out in a foundry company and later in a heat treatment company.

MATERIALS AND METHODS

The chemical composition for the study was selected based on a previous study. It was analyzed using a spark type optical emission spectrometer, table 4 shows the chemical composition. In each Y-block, a sample was taken to be austempered and another was kept in as cast condition for later comparison.

The cast iron was produced in a 1500 kg/hr induction electric furnace (Inductotherm/VIP Dual Track® model) with calculated charging materials in five Y-block form seen in figure 12, as per A536-14 standard. The section thickness was 25 mm (16).

Table 4. Chemical Composition.

Element	**C**	**Si**	**Mn**	**P**	**S**	**Cr**	**Ni**	**Al**	**Cu**	**Mg**	**Sn**	**CE**
(%)	3.69	2.42	0.54	0.03	0.01	0.05	0.01	0.02	0.02	0.05	0.04	4.51

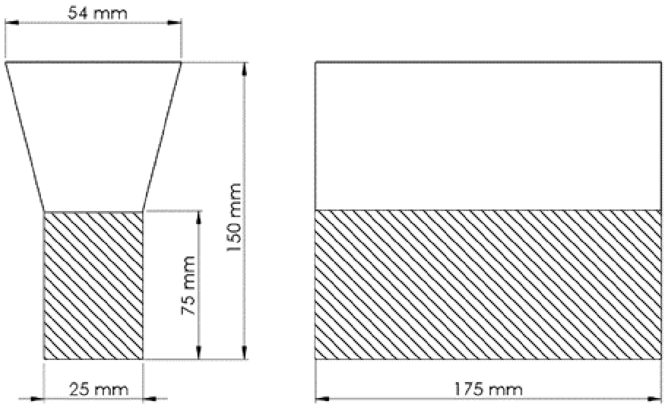

Figure 12. Y-block dimensions.

The austempering heat treatment parameters were selected based on the literature (17–19). The heat treatment cycle started with the material been austenitised at 840°C for 30 minutes. After quenching, subsequently the austempering process was done at 340°C in a quenching tank with salt molten bath based of sodium and potassium nitrate during 30 minutes. Following, the samples were washed in a hot water to remove salt from their surface. The schematic of the heat treatment is shown in figure 13 below.

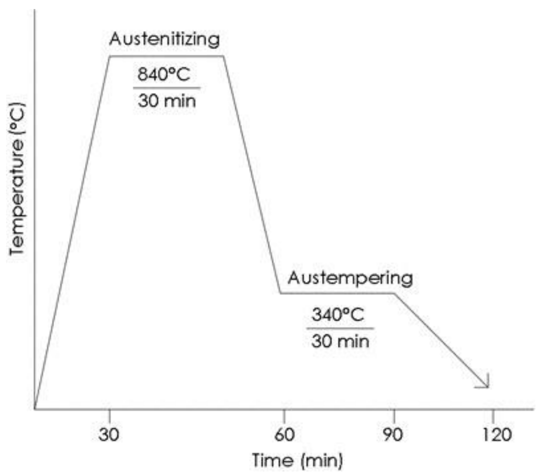

Figure 13. Austempering heat treatment cycle.

The tensile test was carried in a semi-automated machine EMIC 100kN with samples cutted in the lower portion of the Y-blocks. The samples (CP I, CP II, CP III, CP IV and CP V), as show infigure 14 had 58 mm length and 13 mm diameter. The hardness testing wascarried out using a Brinell Hardness Tester at a 3000 kg applied load, using a 10mm diameter steel ball. The sampling was generated at the top of the specimen.

For optical microscopic investigation, the samples were cutted in the other end of the tensile test samples. Later, they were subjected to grinding, polishing and etched using 3% Nital. Scanning electron microscope (SEM) were performed in a SHIMADSU SSX-550 model Superscan. (20–22)

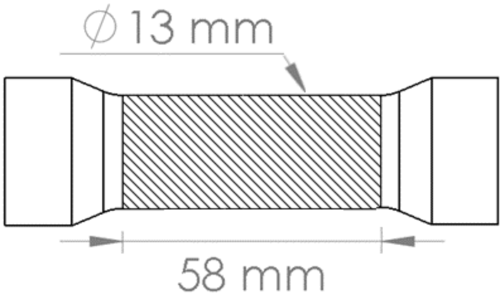

Figure 14. Specimen for tensile test.

The analysis of phases present in the material was performed using x-ray diffraction. XRD is a technique for structural analysis of materials in order to obtain information regarding the structure of the crystal and to quantify the phases present in the alloys. The machine parameters (D8 Advance Bruker®) were: voltage 40 kV, electric current 40 mA, copper tube (Cu), wave (λ): 1,5418Å. The samples were prepared and analyzed through comparison with literature using Origin Software. (23–25).

RESULTS AND DISCUSSION

The microstructure of the as cast condition ductile cast iron shown in Figure 15 presents ferrite, pearlite and graphite in the form of nodules. Figure 16 shows the structure of the material after the austempering process, where it presents graphite nodules surrounded by acicular ferrite in a stabilized austenite matrix. These results are in line with what was expected for this material.

In table 5, average quantity and size of nodules, type, grade and degree of nodularization is presented.

Table 5. Material results.

Material	**Value**
Average nodule count	362 nodule/mm²
Graphite type	I
Graphite Grade	VI
Degree of nodularization	95%
Average size of graphite	35.69 μm

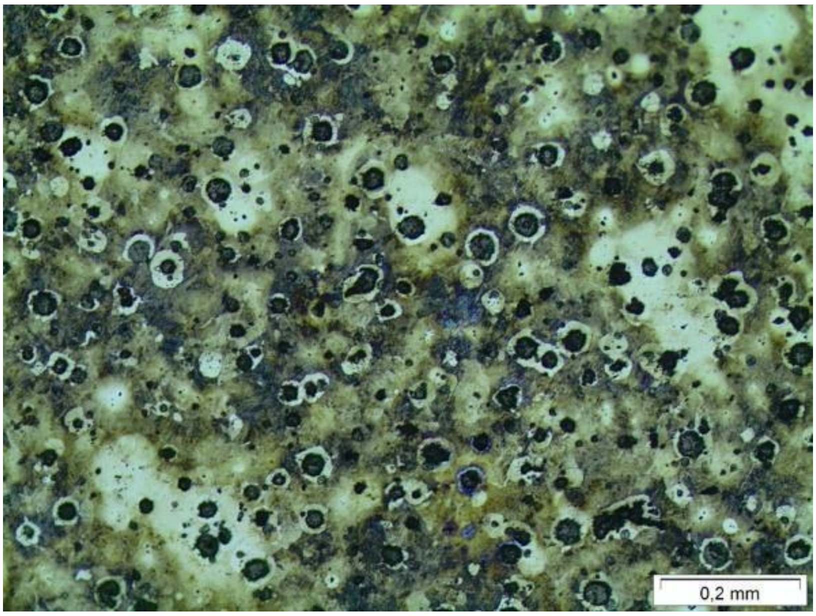

Figure 15. As cast condition – 100x magnification.

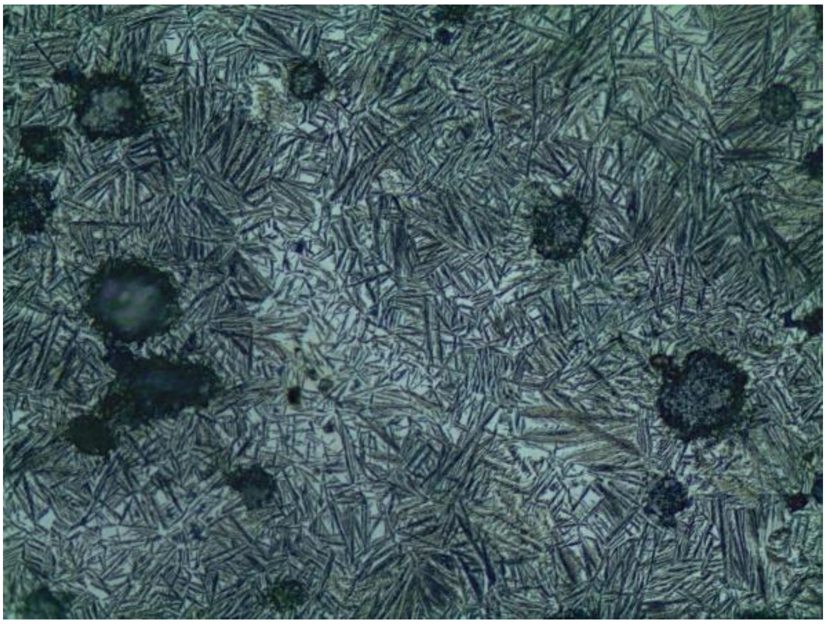

Figure 16. ADI condition – 500x magnification.

The microestruture shown in the figure 17 below, examined through scanning electron microscopy (SEM) presents ductile fracture with dimples confirming with what is expected for this austempered material.

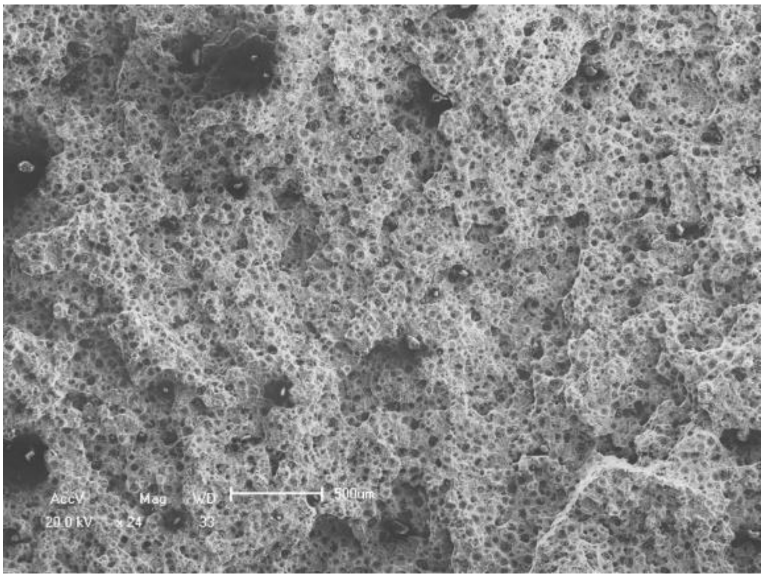

Figure 17. ADI Fracture - SEM microscopy.

The austempering process in this material with a low percentage ofalloying elements showed a great gain in mechanical properties such as tensile and yield strength, when compared to the as cast condition. A low austempering temperature (340°C) provides great strength and hardness when compare with higher temperatures of processing. In this case, it produces a lower ausferritic microstructure (18,23). The graphs show the mechanical tests of the five specimens, figure (18-21), it is possible to observe the great increase in tensile and yield strength when compared to the as cast condition, but at the expense of elongation.

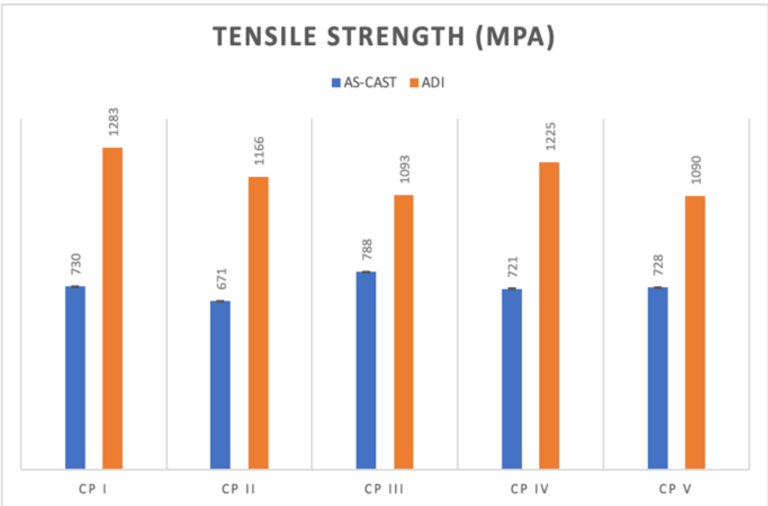

Figure 18. Tensile Strength (MPa) – As cast and ADI condition.

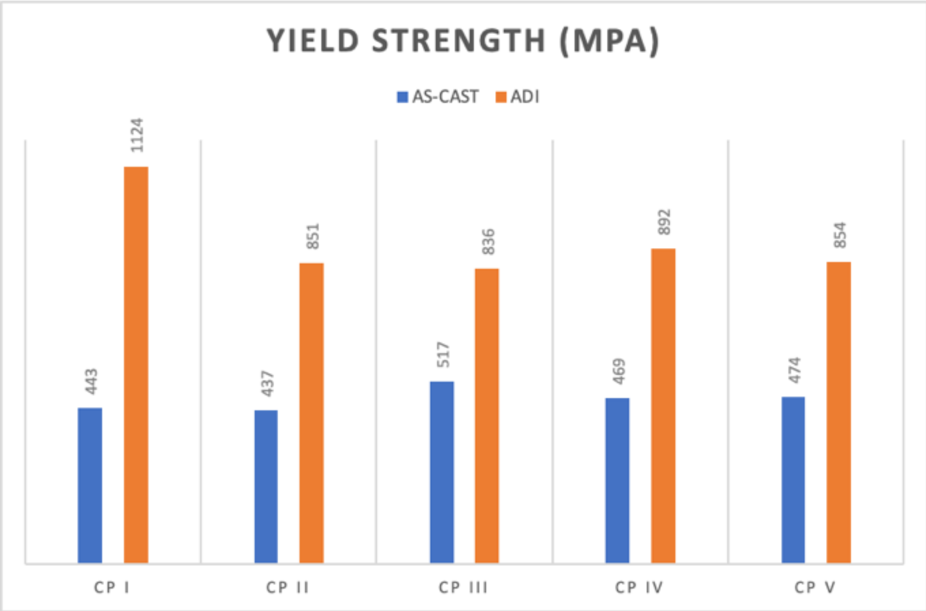

Figure 19. Yield Strength (MPa) – As cast and ADI condition.

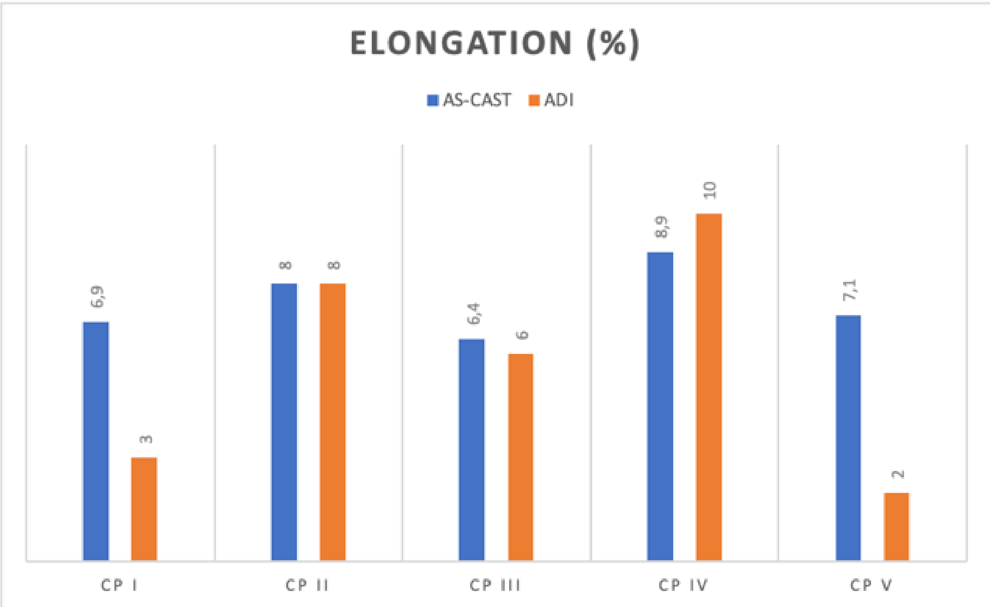

Figure 20. Elongation (%) – As cast and ADI condition.

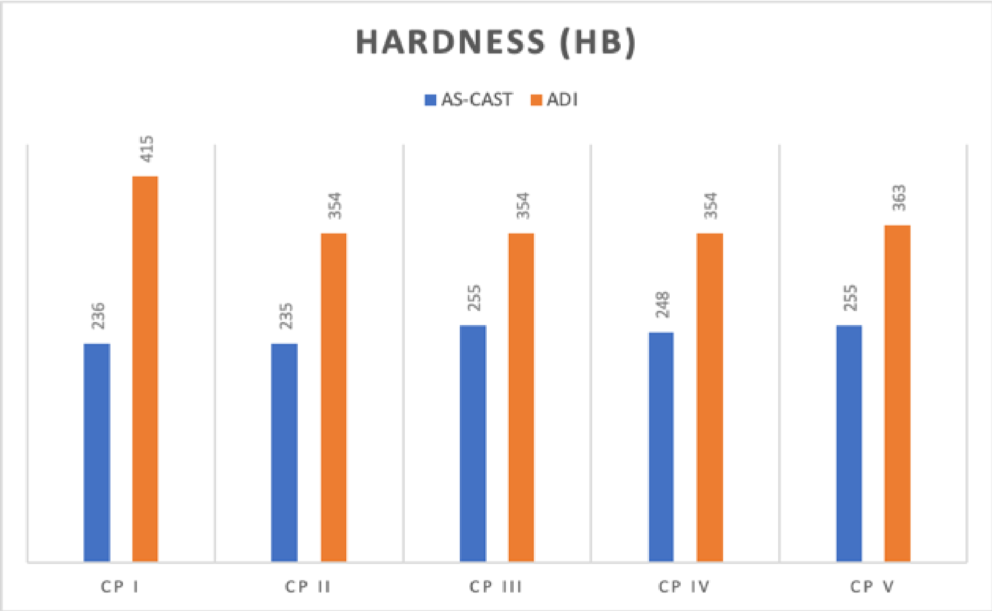

Figure 21. Hardness (HB) – As cast and ADI condition.

Table 6. Standard deviation of graphs.

Standard Deviation	**As Cast**	**ADI**
Tensile Strength (MPa)	41,536	83,858
Yield Strength (MPa)	31,717	120,626
Elongation (%)	0,991	3,346
Hardness (HB)	9,833	26,561

The XRD profiles were analyzed using Origin Pro software, to find out the peak positions planes and it is shown in figure 22. The diffractograms showed high intensity peaks for the ferrite phase (Fe-C), and medium and low intensity peaks for cementite (Fe_3C), consistent with what is expected for the material.

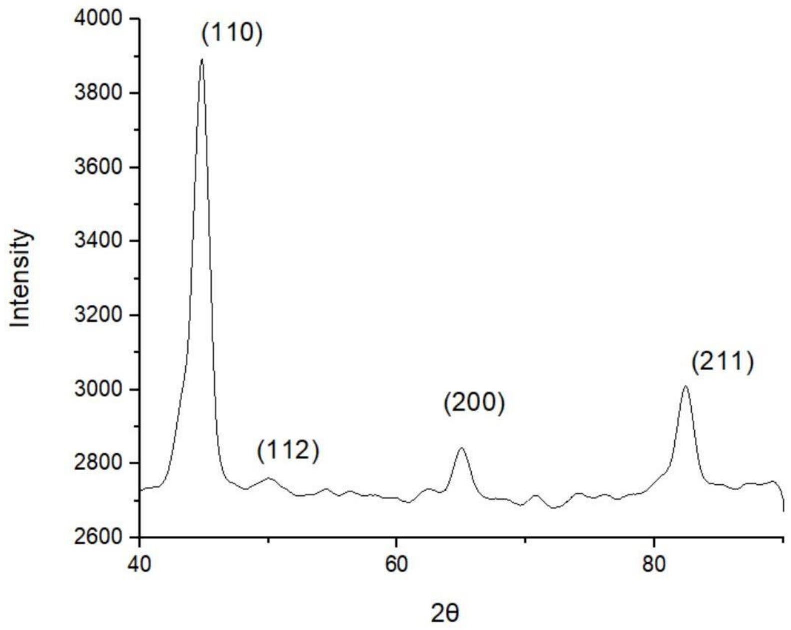

Figure 22. X-ray diffraction for austempered nodular cast iron (ADI).

CONCLUSION

It is possible to achieve with this work the possibility to produce an austempered ductile cast iron with low alloy content. The results of mechanical tests showed a great gain in mechanical properties through the austempering process.

The microstructural results are in agreement with the researched literature, and the x-ray diffraction test showed ferrite and austenite in the microstructure. With the optimization of heat treatment parameters and the non-use, or the reduction in the use of alloying elements, they can become great indicators for the reduction of energy and costs in production.

REFERENCES

1. Brandenberg KR, Hayrynen KL, Agricultural applications of austempered ductile iron. Michigan, USA, 2018.
2. Brandenberg, K.R. Off-highway applications of austempered materials. Michigan, USA, 2002.
3. Kovacs BV. Austempered ductile iron. Fact and ficition. Vol. 80. 1990, p.

38-41.

4. Warrick RJ, Althoff P, Druschitz AP, et al. Austempered ductile iron castings for chassis applications. SAE Tech Pap. p. 724, 2000.
5. Harding RA. The production, properties and automotive applications of austempered ductile iron. Kov Mater. 2007, p. 1-16.
6. Voigt RC. Austempered ductile iron - processing and properties. Cast Met. 1989, p. 71-93.
7. Keough JR, Hayrynen KL, Popovski V, et al. Agricultural applications of austempered iron and steel components. Cast Met. 2009, p. 28-31.
8. Guesser WL, Koda F, Martinez JAB, et al. Austempered ductile iron for gears. SAE Tech Pap. 2012.
9. American Society for Testing and Materials (ASTM). Standard Specification for Austempered Ductile Iron Castings. West Conshohocken: ASTM; 2016. Standard No. A897/897M – 2016.
10. Konca E, Tur K, Koç E. Effects of alloying elements (Mo, Ni, and Cu) on the austemperability of GGG-60 ductile cast Iron. Metals (Basel). 2017, p. 1-9.
11. Eric O, Sidjanin L, Miskovic Z, Zec S, Jovanovic MT. Microstructure and toughness of CuNiMo austempered ductile iron. Mater Lett. 2004, p. 22-23.
12. Batra U., Ray S., Prabhakar S.R. The influence of nickel and copper on the austempering of ductile iron. J Mater Eng Perform. 2004, p. 64.
13. Bosnjak B., Radulovic B., Pop-Tonev K, et al. Influence of microalloying and heat treatment on the kinetics of bainitic reaction in austempered ductile iron. J. Mater Eng. Perform. 2001, p. 203.
14. Keough J.R. Austempered Ductile Iron (ADI) – A Green Alternative. Trans Am Foundry Soc. 2011; p. 591.
15. American Society for Testing and Materials (ASTM). Standard specification for austenitic ductile iron castings. West Conshohocken: ASTM; 2019. Standard No. A536 – 2019.
16. Pereira L., Belle MR., Pasini WM, et al. Determination of the process

window of austemper treatment to obtain ADI through neural network simulation. 2018.

17. Sellamuthu P, Samuel DGH., Dinakaran D, et al. Austempered ductile iron (ADI): Influence of austempering temperature on microstructure, mechanical and wear properties and energy consumption. Metals. 2018, p. 8.
18. American Society for Testing and Materials (ASTM). Standard Specification for Austempered Ductile Iron Castings. West Conshohocken: ASTM; 2010. Standard No. E112 – 2010.
19. International Organization for Standardization (ISO). Determination of tensile properties Geneva: ISO; 2010. Standard No. 527-2 – 2012.
20. American Society for Testing and Materials (ASTM). Standard Specification for Austempered Ductile Iron Castings. West Conshohocken: ASTM; 2010. Standard No. E8/E8M – 2010.
21. Erić O, Rajnović D, Sidjanin L, Zec S, et al. An austempering study of ductile iron alloyed with copper. J Serbian Chem Soc. 2005, p.70.
22. Panneerselvam S, Putatunda SK, Gundlach R, et al. Influence of intercritical austempering on the microstructure and mechanical properties of austempered ductile cast iron (ADI). Mater Sci Eng A. 2017, p. 72–80.
23. Vidal F. D., Análise de estrutura e propriedades mecânicas de um ferro fundido nodular em processo de fundição produzido pela técnica de imersão de sino. 2013.

CONCLUSÃO

Os resultados demonstram a viabilidade da obtenção de uma composição química de baixo custo que atende a norma ASTM A897/897M – 2016, sendo possível ser austemperada e atingindo assim a microestrutura desejada. Uma ferramenta importante para o desenvolvimento foi a utilização de redes neurais artificiais. Dessa forma é possível verificar uma redução de até 49% no valor da liga produzida quando comparada com referências bibliográficas pesquisadas.

Ensaios mecânicos, como de tração e dureza comprovaram valores acima dos mínimos solicitados a partir da Grade 2 1050/750/07 solicitados em norma. Ensaios ópticos, de microscopia eletrônica de varredura e de difração de raio X, confirmaram a formação de estrutura ausferrítica conforme esperado para o material.

Conclui-se então que através do proposto, foi dimensionado uma otimização de processo, levando à redução de custos, menor utilização de recursos naturais e de energia sem a necessidade de modelos empíricos de tentativa e erro para aproximar o resultado do desejado. Alimentando a rede com maiores dados anteriormente pesquisados na literatura, uma maior assertividade é encontrada.

TRABALHOS FUTUROS

Análise de resultados mecânico metalúrgicos em diferentes diâmetros de amostras para buscar um entendimento no diâmetro crítico de transformação ausferrítica.

REFERÊNCIAS

1 Souza BV de. Desenvolvimento de ferro fundido austemperado (ADI) em banho de zinco-alumínio. Pontifícia Universidade Católica do Rio Grande do Sul. Porto Alegre; 2015.

2 Balzer ME. Determinação da janela de processo de austêmpera de um ADI sem adição de elementos de liga através de ensaios mecânicos e metalográficos. Universidade Federal de Santa Catarina. Florianópolis; 2003.

3 Keough JR. Austempered Ductile Iron (ADI) - A Green Alternative for India. Michigan; 2011.

4 Konca E, Tur K, Koç E. Effects of Alloying Elements (Mo, Ni, and Cu) on the austemperability of GGG-60 Ductile Cast Iron. Metals; 2017. 21;7:320.

5 Liu JC, Shi SL. Microstructure and mechanical properties of austempered ductile iron (ADI). Foundry Tech. 2006;27(12):1282–5.

6 Junior ARM. Influência dos elementos de liga Cu-Ni-Mo nas propriedades mecânicas e na austemperabilidade do ADI. 2009;143.

7 Mattar AR, Heck S, Lombardi A, et al. Influence of alloying elements Cu, Ni and Mo on mechanical properties and austemperability of austempered ductile Iron. Inter. Heat Treat. Surf. Eng. 2011 Jun 1;5:78–82.

8 Keough JR, Dorn T, Hayrynen KL, Popovski V. Agricultural Applications of Austempered Iron. Metal Cast. Des. and Purch. 2009;4.

9 Keough JR. Austempered Ductile Iron (ADI) – A Green Alternative. Trans. Am. Foundry Soc. 2011;119(11–126):591–9.

10 American Society for Testing and Materials (ASTM). Standard Specification for Austempered Ductile Iron Castings. West Conshohocken: ASTM; 2016. Standard No. A897/897M – 2016.

11 Bhadeshia HKDH, Dimitriu RC, Forsik S, et al. Performance of neural networks in materials science. Mater. Sci. and Tech. 2009 Apr1;25(4):504–10.

12 Ławrynowicz Z, Dymski S. Neural Network Analysis of Tensile Properties of Austempered Ductile Iron. Adv. Mater. Sci. 2008;8(1).

13 Haykin S. Neural Networks: A Comprehensive Foundation. 1st ed. USA:

Prentice Hall PTR; 1994.

14 Bhadeshia HKDH. Neural networks and information in materials science. Stat. Anal. Data Min. 2009;1(5):296–305.

15 Bhadeshia HKDH, Dimitriu RC, Forsik S, et al. Performance of neural networks in materials science. Mater. Sci. and Tech. 2009;25(4):504–10.